

UCSF

UC San Francisco Previously Published Works

Title

Elucidating the Burden of HIV in Tissues Using Multiplexed Immunofluorescence and In Situ Hybridization: Methods for the Single-Cell Phenotypic Characterization of Cells Harboring HIV In Situ

Permalink

<https://escholarship.org/uc/item/4640g614>

Journal

Journal of Histochemistry & Cytochemistry, 66(6)

ISSN

0022-1554

Authors

Vasquez, Joshua J
Hussien, Rajaa
Aguilar-Rodriguez, Brandon
et al.

Publication Date


2018-06-01

DOI

10.1369/0022155418756848

Peer reviewed

Elucidating the Burden of HIV in Tissues Using Multiplexed Immunofluorescence and In Situ Hybridization: Methods for the Single-Cell Phenotypic Characterization of Cells Harboring HIV In Situ

Joshua J. Vasquez*, Rajaa Hussien*, Brandon Aguilar-Rodriguez, Henrik Junger, Dejan Dobi, Timothy J. Henrich, Cassandra Thanh , Erica Gibson, Louise E. Hogan, Joseph McCune, Peter W. Hunt, Cheryl A. Stoddart, and Zoltan G. Laszik

Division of Experimental Medicine, Department of Medicine (JJV, RH, BA-R, TJH, CT, EG, LEH, JM, PWH, CAS); Division of Pulmonary, Critical Care, Allergy, and Sleep Medicine, Department of Medicine (JJV); Department of Pathology (HJ, DD, ZGL); Division of HIV/AIDS, Department of Medicine (TJH, PWH); and Division of Infectious Diseases, Department of Medicine (TJH, PWH), University of California, San Francisco, CA, USA

Summary

Persistent tissue reservoirs of HIV present a major barrier to cure. Defining subsets of infected cells in tissues is a major focus of HIV cure research. Herein, we describe a novel multiplexed in situ hybridization (ISH) (RNAscope) protocol to detect HIV-DNA (vDNA) and HIV-RNA (vRNA) in formalin-fixed paraffin-embedded (FFPE) human tissues in combination with immunofluorescence (IF) phenotyping of the infected cells. We show that multiplexed IF and ISH (mIFISH) is suitable for quantitative assessment of HIV vRNA and vDNA and that multiparameter IF phenotyping allows precise identification of the cellular source of the ISH signal. We also provide semi-quantitative data on the impact of various tissue fixatives on the detectability of vDNA and vRNA with RNAscope technology. Finally, we describe methods to quantitate the ISH signal on whole-slide digital images and validation of the quantitative ISH data with quantitative real-time PCR for vRNA. It is our hope that this approach will provide insight into the biology of HIV tissue reservoirs and to inform strategies aimed at curing HIV. (*J Histochem Cytochem* 66:427–446, 2018)

Keywords

HIV reservoir, quantitative image analysis, tissue fixation

Introduction

The persistent reservoir of HIV is thought to be the key barrier to a cure.^{1,2} Reservoirs of HIV circulating in the blood have been studied extensively, but the reservoirs hidden within tissues are not well described.³ Tissue reservoirs of HIV are thought to exist within immune privileged sites with variable drug penetration, and are likely to be found within tissue resident cells that are less likely to be found circulating in blood, such as T-follicular helper cells.^{4–6} Blood biomarkers to estimate the tissue reservoir of HIV have been proposed but there is no clear evidence that they correlate with the number of persistently infected cells in tissues.^{7,8} Moreover, techniques to assess the

reservoir of HIV in blood, or PCR-based techniques to do so in tissue, do not provide an anatomic framework for

Received for publication July 19, 2017; accepted January 8, 2018.

*These authors contributed equally to this work.

Corresponding Authors:

Joshua J. Vasquez, Division of Experimental Medicine, Department of Medicine, University of California, San Francisco, 1001 Potrero Avenue, Building 3, 6th Floor, Room 601, San Francisco, CA 94118, USA.
E-mail: joshua.vasquez@ucsf.edu

Zoltan G. Laszik, Department of Pathology, University of California, San Francisco, 513 Parnassus Avenue, Room S564B, San Francisco, CA 94143, USA.
E-mail: zoltan.laszik@ucsf.edu

the location of cellular reservoirs and their association with the local immune environment.

RNA and DNA in situ hybridization (ISH) has been used to localize HIV nucleic acids within tissues.⁹ These studies, and more recent data from Fukazawa et al., using RNAscope ISH, show that HIV and simian immunodeficiency virus (SIV) are frequently found within the B-cell follicle consistent with the notion that tissue reservoirs exist within immune privileged sites.⁶ Deleage et al. highlighted the advantages of RNAscope ISH compared with other methods of ISH and described the use of this technique to assess the tissue burden of SIV.¹⁰ In that study, they showed the ability to multiplex RNA and DNA ISH to identify cells that are HIV-DNA positive (vDNA)⁺ and HIV-RNA positive (vRNA)⁺ as well as cells that are vDNA⁺ but vRNA⁻. PCR-based analysis of cell suspensions phenotyped by flow-assisted cell sorting from HIV/SIV-infected tissues have confirmed that reservoirs are found within subsets of T-cells thought to be residing predominantly within the B-cell follicle.^{5,6} Methods have recently been established to simultaneously identify vDNA or vRNA positive cells with a single immunophenotypical marker in situ.^{10,11} However, methods to simultaneously identify vRNA and/or vDNA with multiple phenotypical markers for the characterization of tissue resident subsets of HIV-infected cells have yet to be reported. Multiplexed in situ analysis of nucleic acids and proteins is challenging, mostly due to compatibility issues of various techniques and variation in tissue preparation. It has been shown that appropriate tissue handling and fixation are important for successful ISH.^{12–16} Therefore, we sought to define optimal conditions of fixation for human tissues fitting for both ISH and immunofluorescent (IF) phenotyping. Herein, we provide the first description of a multiparameter IF phenotyping and ISH assay to detect vRNA and vDNA in HIV-infected human tissues. Moreover, we provide a standardized protocol for tissue preparation that is amenable to ISH and tissue-based immunophenotyping. We show that cells harboring vRNA and/or vDNA can be phenotyped by IF, that chromogenic and fluorescent-based techniques can be multiplexed for more complex analysis, and that these approaches can be used to characterize the disposition of HIV infection within human tissues. Finally, we demonstrate that quantitative ISH (qISH) and quantitative polymerase chain reaction (qPCR) from formalin-fixed paraffin-embedded (FFPE) tissues yield comparable results for the HIV-RNA tissue load.

Materials and Methods

Materials

Supplies. Superfrost Plus Microscope Slides (Thermo Fisher; Waltham, MA); Coverslips no. 1 (Corning;

Corning, NY); IMMEDGE hydrophobic barrier pen (Vector; Burlingame, CA); Moist Mark Plus Pen (Cancer Diagnostics; Durham, NC); ProLong Gold Antifade mountant with 4',6-diamidino-2-phenylindole (DAPI; Thermo Fisher); EcoMount (Biocare; Pacheco, CA); paraformaldehyde (PFA) 16% or 32% solution electron microscopy (EM) grade (Electron Microscopy Sciences; Hatfield, PA); xylene (Sigma-Aldrich; St. Louis, MO); 200 proof ethanol (Koptec; King of Prussia, PA); Tris-HCl powder (Calbiochem; Billerica, MA); Tris-Base powder (Thermo Fisher); NaCl powder (Sigma-Aldrich); Tween 20 (Sigma-Aldrich); PBS 1× (Corning); tyramide signal amplification (TSA)-conjugated to fluorescein, Cy3, or Cy5 (Perkin Elmer; San Jose, CA); Deep space black, Warp red, and Vina Green (Biocare); modified Mayer's hematoxylin (Thermo Fisher); Histogel (Thermo Fisher); saline-sodium citrate (SSC) 20× (Thermo Fisher); RNaseZap (Ambion; Foster City, CA); Pure-Link FFPE Total RNA Isolation Kit (Thermo Fisher); RNeasy Micro Kit (Qiagen; Germantown, MD); heat-inactivated fetal bovine serum (FBS; Gemini; Sacramento, CA); Antibody diluent with background-reducing components (Dako; Santa Clara, CA); TaqMan Fast Virus 1-Step Master Mix (Thermo Fisher).

Antibodies.

- (1) Antibodies are diluted in the appropriate ratio of antibody diluent with background-reducing components (Dako).
 - (2) All of the antibodies listed below have been validated for use with the fixation and pretreatment conditions described herein. The use of other antibodies will require optimization.
- Primary antibodies: anti-CD3 [(rabbit) (UCHT1) (Dako) (1:100)]; anti-CD68 [(mouse) (NCL-CD68-KP) (Leica; Buffalo Grove, IL) (1:100)]; anti-CD163 [(mouse) (NCL-CD163) (Leica) (1:100)]; anti-CD21 [(mouse) (2G9) (Thermo Fisher) (1:10)]; anti-p24 [(mouse) (Kal-1, also known as H-11) (Dako) (1:50)]
 - Secondary antibodies: anti-mouse [(DyLight 649) (DL-2649) (Vector) (1:250)]; anti-rabbit [(Alexa Fluor 594) (A21207) (Life Tech) (1:250)]; Polink-1 polymer horseradish peroxidase (HRP) anti-mouse IgG (GBI Labs; Mukilteo, WA)

Advanced Cell Diagnostics (ACD; Newark, CA) RNAscope Probes

- HIV-RNA and HIV-DNA Singleplex assays: V-HIV1-Clade B sense-78 probe pairs (425531); V-HIV-Clade B antisense-78 probe pairs (416111)

- HIV-RNA and HIV-DNA duplex assays: HIV-non-gagpol antisense-C1-40 probe pairs (317711); HIV-gagpol-sense-C2-40 probe pairs (317701)
- 2-Plex positive control (320741)

ACD RNAscope Kits

- RNAscope 2.5 HD Singleplex Red or Brown Kit
- RNAscope 2.5 HD Duplex Reagent Kit
- RNAscope 2.5 HD Custom-Duplex Reagent Kit with dual HRP endpoints
- RNAscope Multiplex Fluorescent Kit, version 2 [requires TSA (Perkin Elmer) and HRP blocker (ACD)]

Buffers and Solutions

- TBS 1×: Tris-HCl 1.5M, Tris-Base 0.4M, NaCl 15 M dissolved in distilled Milli-Q water (MilliporeSigma; Billerica, MA) (pH 7.7).
- Tris-buffered saline with 0.01% Tween 20 (TBST): dilute 10× TBS, prepared as above, to 1× with Milli-Q water, then add 0.01%(w/v) of Tween 20.
- Immunofluorescence (IF) blocking buffer: 10% FBS diluted in 1× TBS.

Fixatives

- 4% PFA: diluted to 16% EM grade PFA to 4% in 1× PBS chilled to 4C.
- 10% neutral buffered formalin (NBF; Cardinal Health; Dublin, OH): This fixative was used on clinical tissues and denotes a 4% formaldehyde solution diluted 1:10 in phosphate buffer that is stabilized by 10–15% methanol. Note, this reagent is not made fresh and may contain PFA breakdown products.
- Zenker's fixative (Ricca; Arlington, TX): distilled water, mercuric chloride, potassium dichromate, sodium sulfate anhydrous.
- B-5 fixative (American MasterTech; Lodi, CA): stock solution: distilled water, sodium acetate, mercuric chloride. Working solution prepared immediately before use: Add 3.2 ml of 32% PFA for every 32 ml of B-5 stock solution.
- Bouin's solution (Ricca): distilled water, formaldehyde, acetic acid, methyl alcohol, picric acid.
- Methacarn (American MasterTech): methanol, chloroform, acetic acid.
- Smart Tube Proteomic Stabilizer 1 (Smart Tube; San Carlos, CA): proprietary formula that contains formaldehyde.

- Z7 (as described by Stylianopoulou et al.¹²): 0.5% zinc chloride, 0.5% zinc trifluoroacetate (17.16 mM), 0.05% calcium acetate, 0.1 M Tris-HCl pH 6.4–6.7.
- Z7 + 16% PFA: Z7, as above, diluted 1:1 with 32% PFA.

Methods

Sample Preparation (For Paraffin-Embedded Tissues Unless Otherwise Specified). The University of California, San Francisco (UCSF) Animal Care and Use Committee approved all work on animal tissues. The UCSF Committee on Human Subjects Research approved all work on human tissues, and all participants provided informed consent. Supplemental Table 1 describes HIV⁺ human tissues.

- Cell Lines: 12 million cells were fixed in 4% PFA at 4C for 48 hr. Fixed cells were then pelleted in Histogel as previously described by Deleage et al.¹⁰
- Thymus/liver (Thy/Liv): Tissues were placed in fixative immediately upon collection. Fixatives used and fixation times varied according to the studies carried out in Table 1 before processing and embedding in paraffin.
- Rectal biopsies: Prospectively collected specimens were fixed in freshly made 4% PFA at 4C for 48 hr. Banked specimens collected before 2011 were placed in 10% NBF at room temperature for an unknown period of time before fixation, followed by dehydration in graded ethanol and paraffin embedding. Banked specimens collected after 2011 were fixed in 4% PFA for ~8 hr at room temperature with subsequent storage in 80% ethanol at room temperature for up to 4 months before processing and embedding.
- Lymph nodes: Banked clinical specimens were fixed in 10% NBF within minutes after collection, and fixation was carried out at room temperature before processing and embedding in paraffin. Fixation times varied between 30 and 51 hr for HIV⁺ specimens and was 16 hr for the HIV⁻ specimen.

Tissue Processing and Embedding

- Paraffin-embedded tissues: After fixation, tissues were processed and embedded in paraffin according to the following protocol: 10% NBF (3 hr 45 min at 40C); 80% ethanol (45 min at 40C);

Table 1. The Optimal Fixation and Embedding Conditions for the Assessment of HIV-RNA and HIV-DNA by RNAscope in Tissues.

Fixation Conditions ¹	Tissue Morphology ²	vRNA Visible/crisp	vRNA Quantity ³	vRNA Quality ⁴	vDNA Visible	vDNA Quantity ³	vDNA Quality ⁵	Post-Fixation ⁶
Bouin's solution	Poor	Yes	4b	2b	Yes	4	1b	No change
B-5	Poor	Yes	1b	1b	No	—	—	No change
Z7	Acceptable	No	—	—	Yes	2	3b	No change
Z7 + 16% PFA	Acceptable	Yes	4b	2b	Yes	4	1a	No change
Zenker's	Poor	No	—	—	No	—	—	No change
Methacarn	Poor	No	—	—	No	—	—	No Change
Smart Tube	Acceptable	Yes	3b	2b	Yes	4	1b	NA
4% PFA 1–2 days	Good	Yes	4b	2b	Yes	4	1	No change
4% PFA 3–7 days	Good	Yes	5	2a	Yes	5	1a	NA
4% PFA 8–18 days	Good	Yes	4b	2b	Yes	5	1a	NA
4% PFA for 1 day at 4C, then 70% ethanol for 1 day	Acceptable	No	—	—	No	—	—	No Change
4% PFA for 1 day at room temperature, then 70% ethanol for 1 day	Good	Yes	3b	2b	Yes	4	1b	NA
4% PFA for 3 days, then 70% ethanol for 1 day	Good	Yes	4b	2b	Yes	5	1b	NA

Abbreviations: PFA, Paraformaldehyde; vRNA, HIV-RNA; vDNA, HIV-DNA.

¹All tissues were fixed for 1 day at 4C and embedded in paraffin unless otherwise specified.

²Tissue morphology was rated as "Good, Acceptable, or Poor."

³The number of cells positive for vRNA or vDNA: 5 = >100, 4 = 99–70, 3 = 69–40, 2 = 39–10, 1 = <10, b = fewer than expected putative virions.

⁴The quality of vRNA-ISH: 1 = cell-associated vRNA but no putative virions, 2 = cell-associated vRNA and putative virions, 3 = putative virions but no cell-associated vRNA, a = signal is sharp and well localized, b = signal is diffuse or poorly localized.

⁵The quality of vDNA-ISH: 1 = large intra-nuclear signal, 2 = small intra-nuclear signal, a = signal is sharp, b = signal is diffuse and poorly localized.

⁶Post-fixation was performed by placing mounted sections in 4% PFA at room temperature for 15 min.

95% ethanol (45 min at 40C); 95% ethanol (45 min at 40C); 100% ethanol (30 min at 40C); 100% ethanol (45 min at 40C); 100% ethanol (45 min at 40C); xylene (45 min at 40C); xylene (60 min at 40C); fresh paraffin (20 min at 62C); paraffin (20 min at 62C); fresh paraffin (45 min at 62C); fresh paraffin (30 min at 62C); embed in fresh paraffin.

Sectioning and Mounting. Paraffin sections were mounted on Superfrost plus slides. Before sectioning, work areas and blades were treated with RNaseZap. Paraffin sections were floated in a Milli-Q water bath before mounting. After mounting, paraffin sections were air-dried at room temperature and remained unbaked until dewaxing.

ISH and IF Staining Protocols

We recommend that multiplexing with IF be avoided for RNA targets visualized by chromogenic endpoints and/or DNA targets utilizing fluorescing chromogens, such as Fast Red. We found that multiplexed ISH-IF staining is optimally performed when assessing DNA targets developed with non-fluorescent chromogens and/or DNA and RNA probes labeled

directly with fluorophores or TSA conjugated to fluorophores.

Slide Preparation

- **Deparaffinization:** Paraffin-embedded slides are warmed at 60C for 1 hr, then immediately dipped into fresh 100% xylene for 5 min at room temperature, twice. Slides are then put into fresh 100% ethanol for 3 min at room temperature, twice. Slides are then air-dried for 5 min. For post-fixation procedures, slides are moved from 100% ethanol to 4% PFA for 10 min at room temperature followed by a 2-min wash in PBS, then air-dried for 20 min.
- **Deparaffinization for samples stained with fluorescent probes:** Protocols for fluorescent staining are modified to avoid drying, which may increase autofluorescence. Tissues are deparaffinized as above but after the final incubation in 100% ethanol, slides are moved to 80% ethanol for 5 min at room temperature, then washed in Milli-Q water for 3 min. Next, samples are removed from water one at a time, and two to four drops of 1× TBS are added to cover the tissue. With the droplet of 1× TBS in place, a hydrophobic barrier pen is drawn

to encircle the tissue. The hydrophobic barrier is then air-dried for 20 min.

- **Cytospins:** Cells are resuspended at a concentration of 2×10^6 cells/ml in PBS. Then, $\sim 0.2 \times 10^6$ cells/cytospin are cytospun at 600 rpm for 10 min. Next, slides with cytospins are air-dried for 20 min, then placed in 4% PFA for 48 hr and air-dried for 10 min before proceeding with ISH.

Singleplex Chromogenic ISH Staining for vRNA or vDNA Using ACD RNAscope 2.5 HD Red or Brown Kits

Pretreatment. After sample preparation, sections receive two to four drops of RNAscope Pretreat 1 (endogenous hydrogen peroxidase blocker, which is a different formulation than the HRP blocker used to block residual HRP on labeled probes) for 10 min at room temperature, then rinsed twice with Milli-Q water. Heat-induced epitope retrieval (HEIR) is performed by boiling slides in RNAscope Pretreatment 2 for 15 min while maintaining the temperature between 98 and 102°C, then washed twice for 2 min in Milli-Q water, followed by a quick dehydration dip into 100% ethanol before air-drying for 5 min. After slides are fully dried, a hydrophobic barrier pen is drawn encircling the tissue, then barrier is air-dried for 20–30 min before adding RNAscope Pretreatment 3 reagent (digestion enzyme) diluted 1:5 in PBS for 15 min at 40°C in an ACD HybEZ hybridization oven. *For experiments including IF, slides are taken directly from 100% ethanol to Pretreatment 3 to avoid drying.* During pretreatment 3, target probes are warmed to 40°C in the HybEZ oven. Slides are washed twice for 2 min in Milli-Q water.

Hybridization. Next, two to four drops of pre-warmed probes for RNA or DNA targets are added. For RNA-ISH experiments, slides are incubated for 2 hr at 40°C in a HybEZ oven. For DNA-ISH experiments, slides are incubated for 15 min at 60°C in a HybEZ oven, then quickly transferred to 40°C in a second HybEZ oven overnight (18–21 hr). Slides are then washed twice for 2 min in 1× RNAscope Washing Buffer. *At this point, the protocol can be paused for experiments targeting RNA by placing slides in 5× SSC for overnight storage at 4°C. Sections should be washed twice for 2 min in 1× RNAscope Washing Buffer before resuming protocol.*

Amplification 1–6. Amplification steps are performed as described in the RNAscope 2.5 HD red or brown user manual with the exception that washes between each amplification step are performed with 0.5× as opposed to 1× RNAscope Washing Buffer. After the

final amplification (Amp 6), sections are washed twice for 2 min in TBST.

Signal Development. Amp 6 includes alkaline phosphatase (AP) or HRP labels for red or brown kits, respectively. After the last TBST wash step, probes containing AP labels are developed using Warp Red (Biocare) according to the manufacturer's recommendations for 3 min or 8 min for vRNA or vDNA targets, respectively. Probes labeled with HRP are developed using Deep Space Black (Biocare) according to the manufacturer's recommendations for 3 or 10 min for vRNA or vDNA targets, respectively. Slides are washed once for 2 min in 1× RNAscope Washing Buffer, then quickly dipped in distilled water. At this point, samples either move on to IF staining or are directly counterstained and cover-slipped as described below.

Duplex Chromogenic ISH Staining for vRNA and vDNA Using ACD RNAscope 2.5 HD Duplex Kit. Samples to be stained for two nucleic acid targets are treated as described above in the singleplex protocol until the hybridization step. Here, 50× channel (C) two probes are diluted 1:50 with C1 probes. In this assay, C2 probes will ultimately be AP labeled, and C1 probes will be HRP labeled. Next, two to four drops of pre-warmed and diluted probes are added to the sections. Next, samples with two RNA targets are incubated for 2 hr at 40°C in a HybEZ oven. However, for experiments including DNA targets, slides are incubated for 15 min at 60°C in a HybEZ oven, then quickly transferred to 40°C in a second HybEZ oven overnight (18–21 hr). Slides are then washed twice for 2 min in 1× RNAscope Wash Buffer. *Experiments only targeting RNA can be paused at this point by placing slides in 5× SSC at 4°C, as above.*

Amplifications 1–6. Amplification steps are performed as described in the section above. Development of C2-AP labeled probe: Next, AP labeled probes are detected using Warp Red (Biocare) according to the manufacturer's recommendations for 3 min or 8 min for vRNA or vDNA targets, respectively. Slides are washed in 1× RNAscope Washing Buffer.

Amplifications 7–10. Amplifications 7–10 to amplify C1 signals are carried out as described in the RNAscope 2.5 HD Duplex Kit user manual with the exception that washes between each amplification step are performed with 0.5× as opposed to 1× RNAscope Washing Buffer. After Amp 6, slides are washed twice for 2 min in TBST.

Development of C1-HRP-Labeled C1 Probe. HRP-labeled C1 probes are detected using Deep Space Black (Biocare) according to the manufacturer's recommendations for 3 min or 10 min for vRNA or vDNA targets, respectively. Slides are washed once for 2 min in 1× RNAscope Washing Buffer, then quickly dipped in distilled water. At this point, samples either move on to IF staining or are directly counterstained and coverslipped as described below.

Duplex Chromogenic ISH Staining for vRNA and vDNA Using ACD RNAscope 2.5 HD Custom-Duplex Kit With Dual HRP Endpoints. This protocol is used for the multiplex detection of a low abundance ISH target, a high abundance ISH target, and IF; or two low abundance ISH targets and IF. Slides are treated as described in the 2.5 HD Duplex kit protocol with the following exceptions.

Development of C2-Low Abundance Signal. Here, C2 is used to visualize vDNA using ACD 3,3' diaminobenzidine tetrahydrochloride (DAB) Brown reagents and are allowed to develop for 15 min. Alternatively, C2 probes can be developed with TSA-fluorescence. For our experiments, vDNA is visualized using TSA-Cy5 at a dilution of 1:3000, according to the manufacturer's instructions, and incubated for 15 min at room temperature. *Dilutions and incubation times of TSA-fluorescence may vary by protocol.* Slides are then washed twice for 2 min in 1× RNAscope Washing Buffer. Next, two to four drops of HRP blocker are added to the sections and incubated for 15 min at 40C in the HybEZ oven. Slides are washed twice for 2 min in 1× RNAscope washing buffer. Slides then move on to amplifications 7–10 as above.

Development of C1-High Abundance Signal. Here, C1 is used to visualize vRNA using TSA-FITC at a dilution of 1:5000, according to the manufacturer's instructions, and incubated for 15 min at room temperature. Slides are then washed for 2 min in 1× RNAscope Washing Buffer. At this point, samples either move on to IF staining or are directly counterstained and coverslipped as described below.

Fluorescent ISH for Multiple RNA Targets Using RNAscope Multiplex Fluorescent Reagents [Requires TSA (Perkin Elmer) and HRP Blocker (ACD)]. We do not recommend this protocol for the visualization of vDNA. Tissues are treated exactly as described in the sections above, taking into account protocols for fluorescently stained sections with the following exceptions.

Hybridization. This kit allows the multiplex detection of up to three RNA species. Therefore, it will be

necessary to dilute 50× C2 and C3 probes with 1× C1 probes as described by the manufacturer.

Amplification. Amplifications and HRP blocking were performed as described by ACD with the exception that washes between each amplification step are performed with 0.5× as opposed to 1× RNAscope Washing Buffer. TSA-fluorescence dilutions were 1:3000 for all probes, but titration is likely necessary for different applications. Finally, if it is desirable to multiplex this protocol with IF staining, we would recommend washing the slides twice with TBST after the final wash in RNAscope wash buffer and before proceeding with IF staining as described below.

Antibody Staining

For mIFISH, antibody staining described below is performed immediately after the final RNAscope wash and begins with two washes in TBST, as described above.

IF Staining. Sections are incubated with 10% FBS for 30 min at room temperature, followed by a 2 min wash in TBST. Sections are now incubated with primary antibody (dilutions may vary, see above) overnight (16–18 hr) at 4C, then washed twice for 2 min in TBST. Sections are incubated with secondary antibody for 45 min at room temperature, then washed twice for 2 min in TBST. At this point, slides are either immediately coverslipped, as described below, or, if multiplexed with chromogenic labels, are counterstained, then coverslipped using protocols for fluorescently stained sections. Anatomic positive controls and isotype-specific sera negative controls were used for all IF staining procedures as per the Histochemical Society's standard of practice.¹⁷

Counterstaining for Chromogenically Labeled Sections

Sections containing chromogenic labels are counterstained with hematoxylin to aid in bright-field slide scanning and analysis. It should be noted that counterstaining with hematoxylin was found to slightly dampen or shift fluorescence in the FITC channel.

Chromogenic Stained Sections. Sections only containing chromogenic labels are counterstained in modified Mayer's hematoxylin for 15 sec, rinsed in tap water, then blued for 15 sec in TBST, followed by a final rinse in tap water. Slides are then air-dried at 60C, then coverslipped according to instructions below.

Multiplexed Chromogenic and Fluorescent Stained Sections. Sections with multiplexed fluorescent and chromogenic endpoints are counterstained as above, but are not dried at 60°C. Instead, slides are directly moved on to coverslipping after the final tap-water rinse.

Coverslipping

Chromogenic Stained Sections. Slides stained using only chromogenic endpoints were mounted after air-drying with EcoMount using VWR cover glass, no. 1.

Fluorescent Only or Chromogenic + Fluorescent Stained Sections. Protocols including fluorescent labels mounted with ProLong Gold Antifade with DAPI hardset mountant using VWR cover glass, no. 1.

ProLong Diamond mountant and the ACD-HRP-Green chromogen was found to be incompatible with chromogenic and fluorescent multiplexed protocols.

Imaging

Bright-Field Imaging. Slides stained using chromogenic endpoints were imaged by bright-field with the Aperio AT Turbo (Leica) digital whole-slide scanning system using the 40× objective lens (UCSF Department of Pathology).

Fluorescent Imaging. Slides stained using fluorescent endpoints were imaged with the Axio Scan.Z1 (Zeiss) using the 20× objective (University of California, Berkeley Imaging Systems Laboratory).

RNAscope Quantification and Analysis

Whole-Slide Quantitative (Digital) Image Analysis (QIA). Quantitation of RNAscope vRNA signal was assessed by automated whole-slide digital image analysis using Definiens Tissue Studio image analysis software (Definiens AG; Munich, Germany). First, 4- μ m thick FFPE sections of HIV⁺ hilar lymph nodes (HLNs) were stained for vRNA using the RNAscope 2.5 HD Singleplex Red kit, as described elsewhere. Slides were digitized at 40× using the Aperio AT2 digital whole-slide scanning system. In our implementation of the Definiens Tissue Studio Spot Detection System, we first manually applied a region of interest, and then created solutions to automatically identify nuclei, whole cells, and ISH signals. The nuclei were detected by the software using a counterstain (Hematoxylin or DAPI) as a marker for nuclei. The individual cells were identified by the software using simulation mode “grow from nuclei at 5 μ m.” Then, after ISH signal detection, the smallest individual (punctate) signals were classified

as individual dots, and larger irregular signals were classified as clusters (fused dots). Next, individual ISH signals were quantified by dividing the total signal area of a given cluster by the average size of an individual signal. These data were quantified and reported for each individual cell. Initial analysis review showed that the solution picked up tissue artifacts as ISH signal. We were able to exclude the nonspecific signal using the brown chromogen analysis, as vRNA was stained red. To validate the solution and as a quality-control measure, we visually assessed 12 randomly selected high-power fields at 40× before and after the application of the solution for the accuracy of nuclei detection and the accuracy of ISH signal detection. Results are presented as the percent of vRNA positive cells of total number of cells per section. Finally, for a more detailed analysis, cells were subclassified as having one dot, two to five dots, and clusters. The QIA was repeated three times on three separate days using two whole-slide images to assess the reproducibility of the protocol.

Cross-Validation of Whole-Slide Digital Imaging Analysis to qPCR. To estimate the number of vRNA transcripts, we first assessed the average size of an individual dot and then quantified the total area of vRNA-ISH signal. Assuming that a single dot represents a single transcript, we estimated the number of individual transcripts required to produce a signal encompassing the total area of vRNA signal within the 4- μ m section. Then, qPCR for HIV-RNA was performed on tissue sections from the same FFPE blocks as described below. Then, qPCR results were normalized to a 4- μ m section thickness and reported as means.

RNA Isolation From FFPE Sections

One or two slices of 10- μ m thick sections of two different FFPE HIV⁺ HLNs were used to extract total RNA, that is, RNA was isolated from two tubes for each sample, either tube containing one or two sections. Rapid purification PureLink FFPE Total RNA Isolation Kit (Thermo Fisher) was used according to the manufacturer's recommendations. Total RNA was extracted using a master mix of 790 μ l TRIzol and 10 μ l glycogen. The tissue samples were homogenized in 800 μ l of the TRIzol/glycogen mix using a power homogenizer making sure the sample volume was well within 10% of the volume of the TRIzol Reagent used for homogenization. After incubating the homogenized mixture at 15–25°C for 5 min, 160 μ l chloroform was added for phase separation. The mixture was vortexed vigorously for ~15 sec and incubated at 15–25°C for 2–3 min, followed by centrifugation 12,000 \times g for 15

min at 4°C. The aqueous phase was removed and used for RNA extraction using RNeasy Micro Kit (Qiagen). The RNA quantity was determined with a Thermo Scientific NanoDrop ND-2000 UV-Vis Spectrophotometer. The concentration of the RNA varied between 348 and 454 ng/μl in the samples.

HIV-RNA and HIV-DNA qPCR

HIV-RNA. Unspliced HIV-1 RNA was quantified using a TaqMan real-time PCR (or qPCR) method based on previously described primer and probe sequences that amplify a conserved region in the long terminal repeat (LTR)/gag region specific to nearly all group M HIV-1 sequences.¹⁸ Briefly, 10 μl of RNA from each tissue section extract (348–454 ng/μl) was added to 10 μl of TaqMan Fast Virus 1-Step Master Mix (Thermo Fisher), incorporating forward primer, 5'-TACTGACGCTCTCG-CACC; reverse primer, 5'-TCTCGACGCAGGACTCG; and probe, 5'-FAM-CTCTCTCCTTCTAGCCTC-MGB, as per manufacturer's protocol, followed by thermocycling with an annealing temperature of 60°C using the LightCycler 96 system (Roche; Pleasanton, CA). Reactions were run in duplicate, and absolute RNA copy numbers were determined based on serial dilutions of a standard curve. Non-template controls were incorporated into each PCR experiment. The vRNA copy number was normalized for the section thickness and the amount of input RNA.

Total HIV-1 DNA was quantified using a qPCR method as we have previously described in detail.¹⁹ The primer and probe sequences were identical to the unspliced HIV-1 RNA assay, detailed above. Briefly, 10 μl of DNA from each tissue section extract was added to 10 μl of TaqMan Universal PCR Master Mix (Thermo Fisher) as per manufacturer's protocol, followed by thermocycling with an annealing temperature of 60°C using the LightCycler 96 system. Reactions were run in duplicate, and absolute DNA copy numbers were determined based on serial dilutions of a standard curve. DNA copy number was normalized using co-amplification of a conserved region of the human *CCR5* gene using the TaqMan Universal PCR Master Mix, as previously published.¹⁸ Each human cell contains two copies of this diploid gene. Non-template controls were incorporated into each PCR experiment.

Results

Controls for the Detection of HIV Nucleic Acids by ISH Using RNAscope

The ACH2 cell line, known to harbor multiple copies of inducible HIV provirus and predictable levels of HIV

transcription at baseline, was used as a quantitative control for the detection of HIV nucleic acids.^{20,21} Four-μm-thick sections of FFPE cell blocks prepared from 12 million unstimulated/uninduced ACH2 cells were stained for either vRNA (black) and vDNA (red) (Fig. 1A) or with a scrambled sequence probe set (Fig. 1B), as a negative control. Approximately 10% of the cells showed strong confluent cytoplasmic signal of vRNA (e.g., confluent signals filling the cytoplasm) while most of the remaining cells had only one or a few individual punctate dots scattered throughout the cytoplasm, consistent with a lesser amount of vRNA content. When staining for vDNA, most cells displayed one to two vDNA signals per nucleus. Background staining with the scrambled probe sets for vRNA and vDNA (Fig. 1B) was negligible. To assess potential differences in the staining properties between tissues and cell blocks, we next analyzed FFPE Thy/Liv tissue implants from HIV⁺ (Fig. 1C and D) and HIV⁻ (data not shown) humanized bone-marrow/liver/thymus (BLT) mice. As in the case of the ACH2 cells, individual cells in the HIV⁺ Thy/Liv implant showed variable levels of vRNA, and some showed both vDNA and vRNA; scrambled probe sets revealed no staining for vRNA and only negligible staining for vDNA (Fig. 1D). The vRNA staining from HIV⁻ controls revealed no background staining, but sections stained for vDNA did show very low levels of background (data not shown). Four-μm-thick FFPE sections do not include the entire area of an average nucleus that has a diameter of ~10 μm. Therefore, staining for vDNA on a single section may only identify a fraction of the vDNA present in the total population of represented cells. To test this hypothesis, we stained a cytospin of formalin-fixed unstimulated/uninduced ACH2 cells for vDNA (Fig. 1E), which would be expected to assess an entire nucleus. Indeed, the cytospin demonstrated cells with multiple (>5) vDNA events in a single nucleus while the 4-μm section (Fig. 1A) demonstrated <3 vDNA signals per nucleus. In addition, qPCR for total vDNA performed on unfixed ACH2 cells from the same passage as the cytospin revealed ~0.5 copies of vDNA/cell.

The Importance of Fixation for ISH (RNAscope) Based Detection of HIV Nucleic Acids

Thy/Liv tissues from HIV⁺ and HIV⁻ BLT humanized mice were used to determine optimal conditions of tissue fixation and processing for RNAscope ISH. All HIV⁺ mice had similar levels of plasma HIV-RNA (range = 4.0–4.5 log₁₀ copies/100 μl). To test the impact of eight various tissue fixatives (Table 1) on the ISH signal, fresh Thy/Liv tissues from HIV⁺ (n=8) and HIV⁻ (n=8) BLT humanized mice were first sliced into

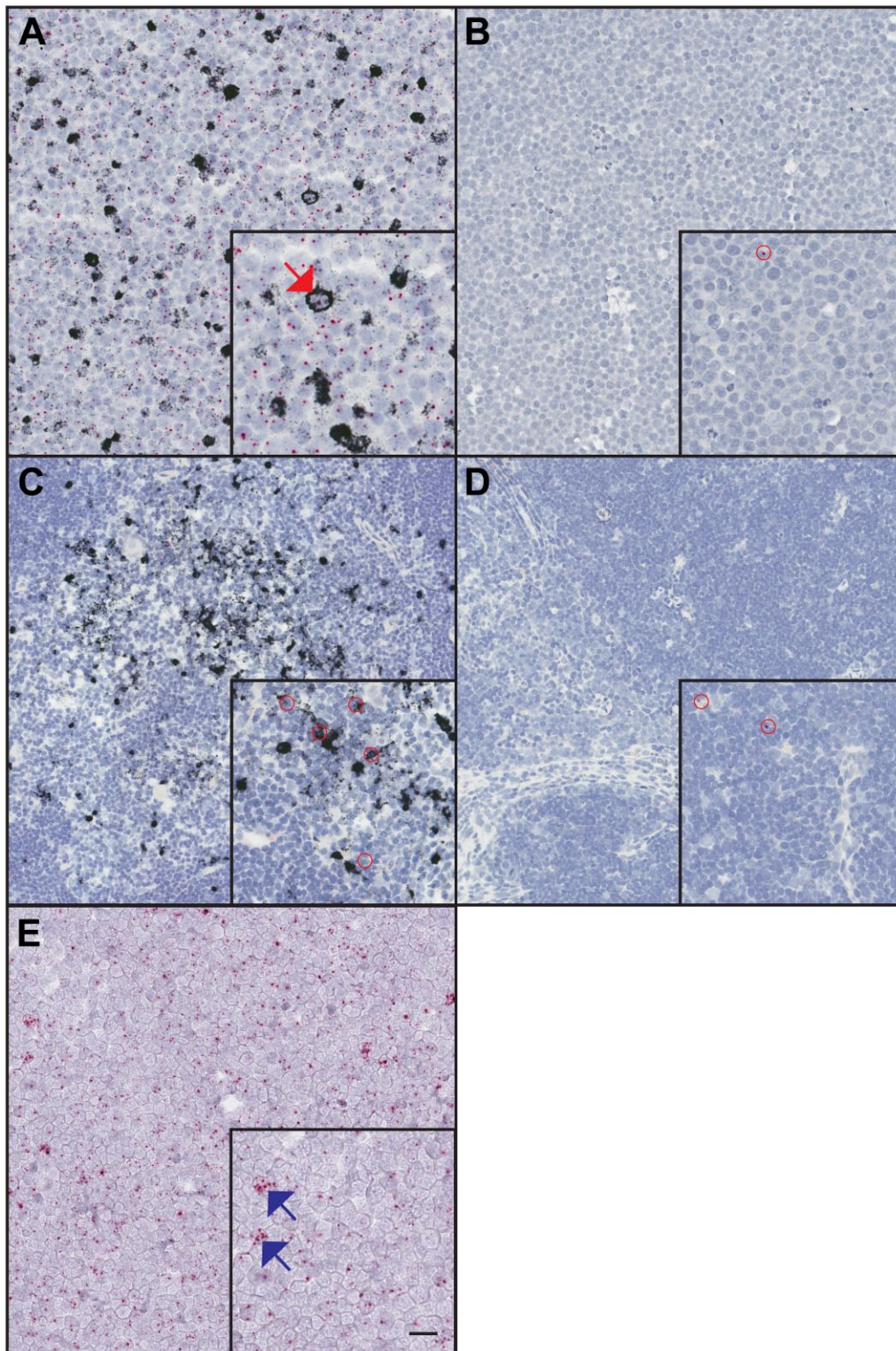


Figure 1. Detection of vRNA and vDNA by ISH using RNAscope. ACH2 cells (A and B) and Thymus/Liver implants from NSG-BLT mice 9 weeks after intraperitoneal inoculation with HIV-1 JR-CSF (C and D) were tested with the RNAscope 2.5 HD Duplex Reagent Kit, using probes for vRNA and vDNA (A and C), or scrambled sequence probes for vRNA and vDNA (B and D), vRNA (black), vDNA (red), and nuclei (blue). A cytospin of ACH2 cells are stained for vDNA (E). The red arrow in A shows a vDNA⁺/vRNA⁺ cell. Red circles in C highlight vDNA. vDNA background was seen in B and D (shown by red circles). The blue arrow in E shows cells with multiple vDNA signals. Main images are at 12 \times magnification, and inset images at 40 \times . Scale bar for inset image = 20 μ m. Abbreviations: vRNA, HIV-RNA; vDNA, HIV-DNA; ISH, in situ hybridization; NOD, nonobese diabetic; SCID, severe combined immunodeficiency; NSG, NOD SCID gamma; BLT, bone-marrow/liver/thymus.

~15 mm³ pieces; each piece was fixed for 1 day at 4C in one of the eight fixatives, embedded in paraffin, and stained by ISH for vRNA and vDNA. Each condition was tested twice using tissues from two different animals, and a minimum of two sections were evaluated from each block. All samples of FFPE Thy/Liv tissues from HIV⁺ mice were found to have large quantities of vRNA and vDNA by ISH and excellent tissue morphology. Because none of the non-formaldehyde-containing fixatives showed evidence of vRNA-ISH signal, the next round of testing was designed to assess the impact of length of fixation (1, 2, 3, 4, 8, and 14 days) only in 4% PFA-fixed tissues. Testing the impact of temperature (4C vs. room temperature) during fixation on ISH was also considered; however, we chose to continue systematic testing only at 4C given previous reports of decreased RNA degradation when fixation or storage is carried out at 4C versus room temperature.^{22,23} Fixation times between 3 and 7 days at 4C showed similar results for vRNA-ISH and vDNA-ISH, while fixation times <2 days or >7 days showed slightly decreased vRNA signal with minimal or no impact on the vDNA signal. It was also noted that the crispness of the vRNA and vDNA signal was slightly decreased at fixation times <3 days or >7 days. Limited testing performed on PFA-fixed Thy/Liv tissues from HIV⁺ mice to address the impact of PFA fixation at room temperature versus at 4C on the ISH signal for samples fixed for 1, 2, 3, and 4 days showed a somewhat superior vRNA-ISH signal at room temperature for time periods <2 days; however, no appreciable difference in the staining intensity was noted for samples fixed for 2 days or longer. Finally, results of PFA fixation were replicated twice for short fixation times (1 day) and longer fixation times (14 days) in dedicated experiments in which Thy/Liv tissues were bisected and one half, fixed for 1 or 14 days, was compared with fixation for 3 days. In each case, fixation at 3 days showed the sharpest ISH signal, lowest background, and most detail of individual punctate dots of vRNA-ISH signal thought to be putative virions. In addition, this method of tissue preparation proved to work well in HIV-infected rectal biopsies (Supplemental Table 1) stained by RNAscope for vRNA housekeeping gene transcripts [peptidylprolyl isomerase B (*PPIB*) and RNA polymerase II subunit A (*POLR2A*)] (Fig. 2A and B). To control fixation times in formalin during specimen transport before embedding, a subset of specimens was transferred to 70% ethanol for 1 day after completion of fixation in 4% PFA, a practice commonly applied to specimens intended for immunohistochemistry. We found that tissues stored in ethanol that had undergone PFA fixation times of ≤1 day at 4C demonstrated an absence of ISH signal. However, tissues fixed in

PFA for 1 day at room temperature and 3 days at 4C showed ISH signal even after storage in ethanol for 1 day. The deleterious effects of ethanol on ISH were again demonstrated by experiments where RNAscope ISH was performed for vRNA or *PPIB* and *POLR2A* on historical samples of rectal biopsies from six HIV-infected viremic patients that were either fixed at room temperature for a long period of time (weeks to months) in 10% NBF (three cases, showing adequate ISH staining; Fig. 2C and D) or for a short time (8 hr) at room temperature in 4% PFA, followed by prolonged storage in ethanol (three cases, showing poor ISH staining; Fig. 2E and F) and then followed by processing and embedding in paraffin. The protocol exposing tissues to prolonged ethanol after formaldehyde-based fixation had inferior staining. All six of these tissue blocks were similarly embedded and stored together, but the three cases with prolonged storage in ethanol, showing poor ISH staining, were collected more recently (after 2011) whereas the other three cases were collected before 2011.

Chromogenic-Based ISH Poses an Optical Barrier to IF Phenotyping of vRNA Positive Cells

Next, we sought to immunophenotype cells positive for HIV nucleic acids. Four-μm-thick sections of FFPE cell blocks prepared from 12 million of unstimulated ACH2 cells that were fixed for 3 days in 4% PFA at 4C were stained for vRNA using Fast Red, a fluorescent chromogen, followed by IF detection of CD3 (Fig. 3A–D). While the great majority of the vRNA⁻ cells were found to be CD3⁺ and vRNA⁺ cells with low-grade (dotted) positivity were all CD3⁺, cells with strong confluent vRNA signal were uniformly negative for both CD3 and the fluorescent nuclear stain, DAPI (compare Fig. 3B and D). We hypothesized that the chromogenic precipitate from RNA-ISH created an optical barrier, thereby impeding the transfer of light across cells that were strongly positive with RNA-ISH, and eclipsing the IF signals. This hypothesis was confirmed by multiplexed chromogenic staining for vRNA and vDNA with IF-immunophenotyping using Thy/Liv tissue sections (Fig. 3E–J), demonstrating that vDNA⁺ cells, with a smaller footprint of chromogenic signal elicited by single-copy intra-nuclear provirus, were positive by IF while cells with heavy vRNA load could not be phenotyped by IF (compare Fig. 3E and J). Although we suspect that this is likely a commonly confronted problem, such an optical barrier has not, to our knowledge, been formally described in the literature.

To overcome this optical barrier to performing IF phenotyping on vRNA⁺ cells with heavy RNA load, we attempted to use a fully fluorescent platform first with

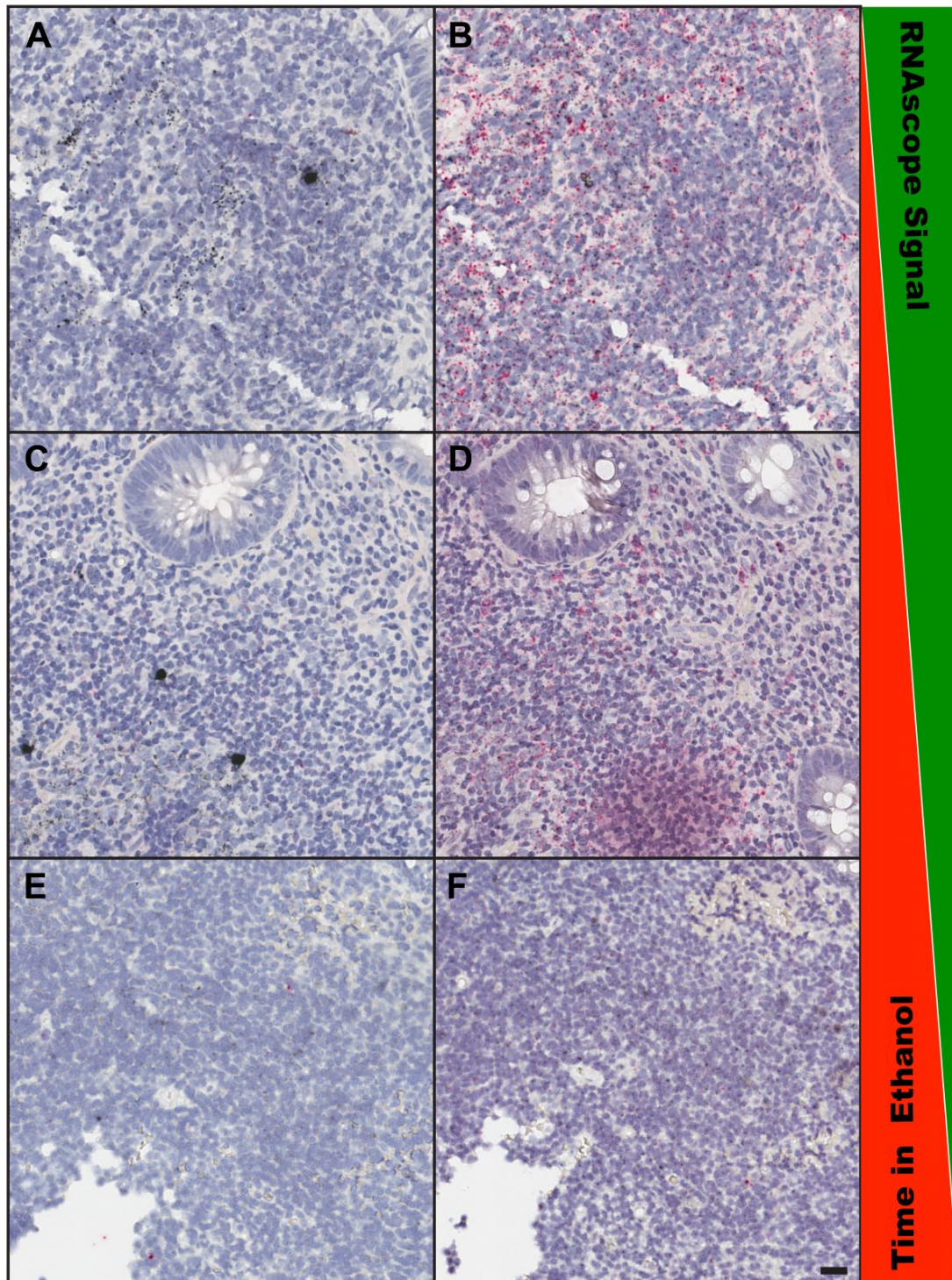


Figure 2. The importance of fixation for RNAscope-based detection of HIV nucleic acids in human gut tissues. Rectal biopsies from HIV⁺ viremic donors were collected and fixed using our optimized protocols (A and B); tissues collected before 2011 were fixed in 10% NBF for days to weeks (C and D); and tissues collected after 2011 were fixed in 4% PFA for ~8 hr with subsequent prolonged exposure to ethanol (days to weeks) before embedding (E and F). Panels A, C, and E were stained for vRNA (black) and nuclei (blue). Panels B, D, and F were stained for housekeeping gene transcripts *PPIB* (red) and *POLR2A* (black); nuclei (blue). Optimally fixed samples show superior staining for vRNA (A) and housekeeping gene transcripts (B). The green and red gradient bars to the right highlight the relationship of time in ethanol with RNAscope signal quality. Images are at 12 \times and scale bar = 20 μ m. Abbreviations: NBF, neutral buffered formalin; PFA, paraformaldehyde; *PPIB*, peptidylprolyl isomerase B; *POLR2A*, polymerase II subunit A; vRNA, HIV-RNA.

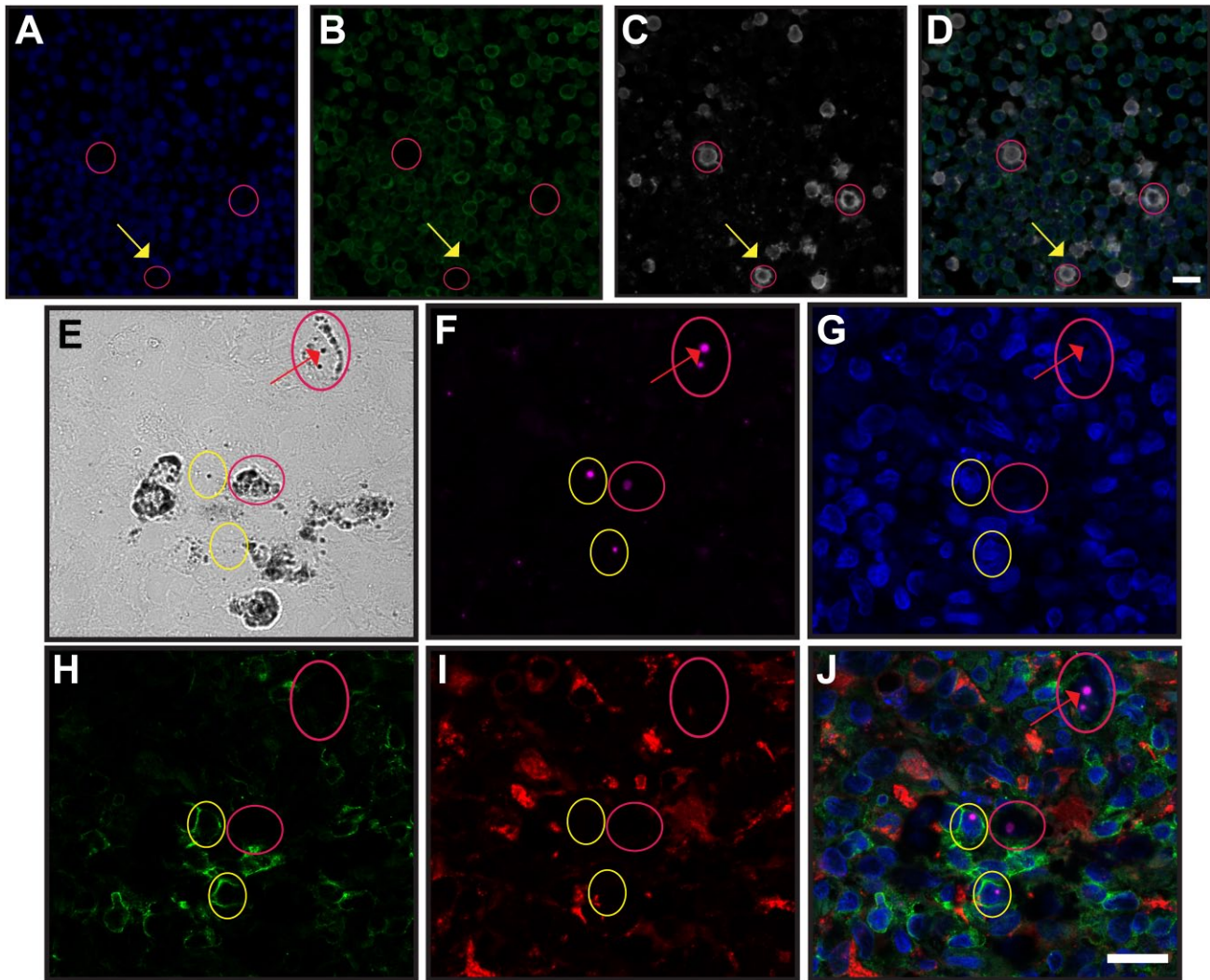


Figure 3. Chromogenic ISH poses an optical barrier to immunofluorescent phenotyping of $vRNA^+$ cells with heavy $vRNA$ load. $CD3^+$ ACH2 cells were stained for DAPI (IF, blue, A), CD3 (IF, green, B), $vRNA$ (ISH, Fast Red chromogen-white, ISH signal is shown via fluorescent visualization, C), and overlay (D). The red circles in A–D highlight $vRNA^+$ cells that show no apparent CD3 staining and significantly dampened nuclear staining. An HIV⁺ Thymus/Liver implant section was stained for $vRNA$ and $vDNA$ using chromogenic ISH; and CD3, CD68, and DAPI using IF (E–J). Visualization of $vRNA$ (Deep Space Black chromogen) and $vDNA$ (Fast Red chromogen; transmitted light, E); $vDNA$ alone (Fast Red chromogen-magenta is shown via fluorescent visualization, F); DAPI (IF, blue, G); CD3 (IF, green, H); CD68 (IF, red, I); and overlay (J). The red circles in E–J highlight $vDNA^+/vRNA^+$ cells with an indeterminate phenotype and dampened fluorescence in locations coinciding with $vRNA$ staining. The yellow circles in E–J highlight $vDNA^+/vRNA^-/CD3^+$ cells. Scale bar = 20 μm . Abbreviations: ISH, in situ hybridization; DAPI, 4',6-diamidino-2-phenylindole; IF, immunofluorescence; $vRNA$, HIV-RNA; $vDNA$, HIV-DNA.

ACD's fluorescent-ISH kit with probes conjugated to fluorophores (data not shown) and then with ACD's 2.5 Brown HRP-based kit followed by TSA conjugated to a fluorescent label, followed by multiplex IF staining for immunophenotyping. Figure 4A (DAPI), 4B ($vRNA$ -TSA-fluorescence), 4C (CD3-IF), and 4D (overlay of $vRNA$, CD3, and DAPI) show multiplex IF and ISH (mIFISH) staining performed on a single section of rectal tissue from a viremic patient featuring clear colocalization of $vRNA$ with an immunophenotypical

marker. Both ACD's fluorescent-ISH kit and the TSA-fluorescence approach were successful in resolving phenotypes of $vRNA$ positive cells by IF; however, when using the fluorescent-ISH kit, we were unable to achieve adequate $vDNA$ signal, which we suspected was due to fewer amplification steps when compared with the chromogenic-based ISH kits (four compared with six amplifications). However, TSA-fluorescence in the context of the RNAscope 2.5 Brown kit was successful in resolving $vDNA$ signals and with specificity

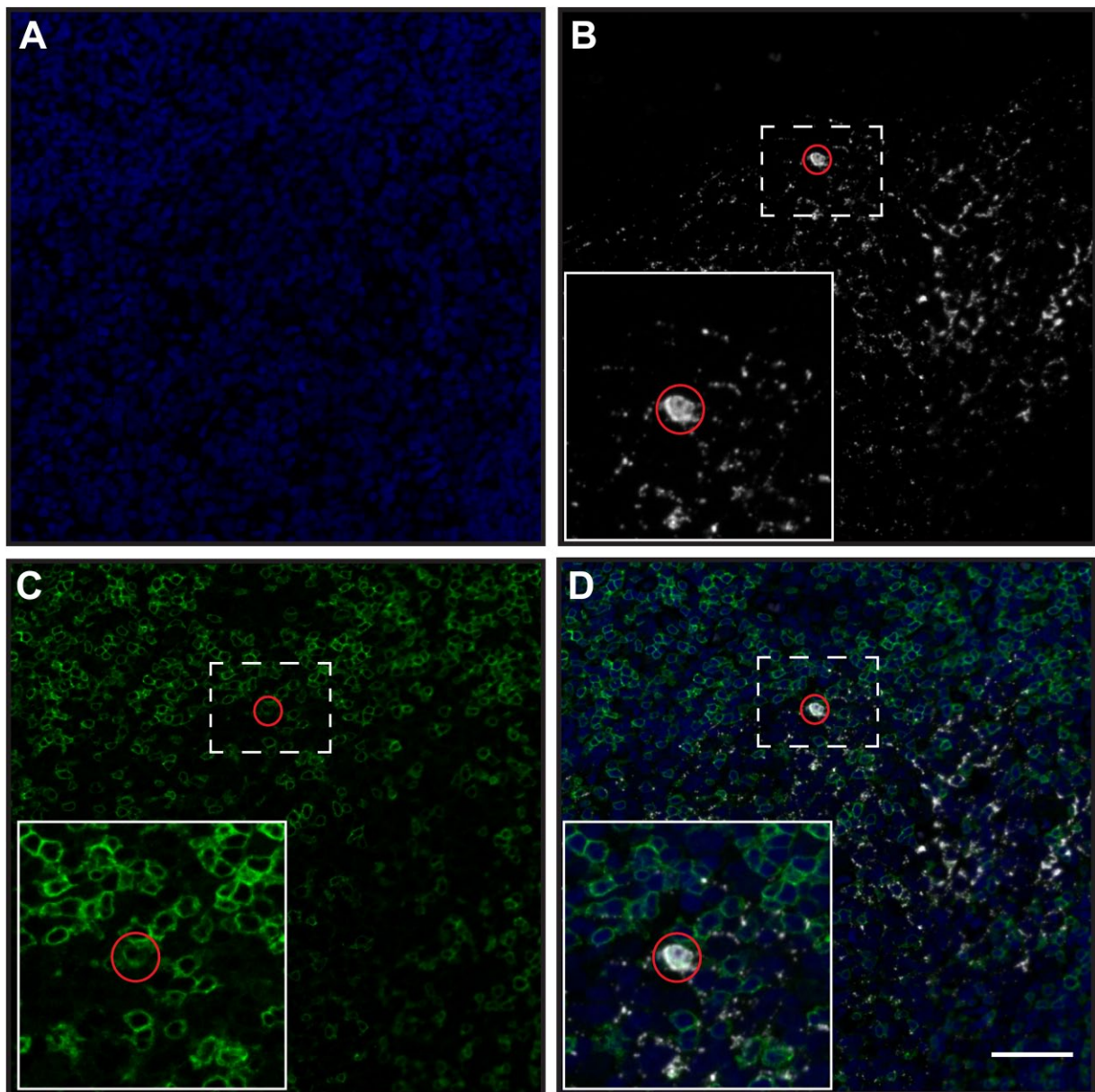


Figure 4. Overcoming the optical barrier of chromogenic ISH. A single FFPE section from an HIV⁺ human rectal biopsy was stained for vRNA-ISH using the RNAscope 2.5 Brown kit, followed by TSA-Cy3 amplification of HRP-labeled vRNA and multiplexed IF for CD3 and CD68/CD163 (all fluorescent mFISH)—DAPI (IF, blue, A); vRNA (TSA-Cy3, white, B); CD3 (IF, green, C); and overlay (D; all fluorescent mFISH; 1 slide, B–D). The red circles in the inset images highlight a single CD3⁺ cell shown to be highly positive for vRNA. Scale bar = 50 μ m. Abbreviations: ISH, in situ hybridization; FFPE, formalin-fixed paraffin-embedded; vRNA, HIV-RNA; TSA, tyramide signal amplification; HRP, horseradish peroxidase; IF, immunofluorescence; mFISH, multiplexed IF and ISH; DAPI, 4',6-diamidino-2-phenylindole.

comparable with that of chromogenic staining for vDNA (Supplemental Fig. 1).

Multiplexed IF Phenotyping of Cells Positive for vRNA and vDNA by mFISH in FFPE Tissues

We were now able to multiplex vRNA and vDNA-ISH using chromogenic labels, and to multiplex vRNA-ISH

and IF using fluorescent labels; however, detection of vDNA along with vRNA and IF signals with ACD's commercially available assay formats remained sub-optimal. We found that it was possible to use TSA-fluorescence to visualize vRNA targets labeled with HRP when duplexed with vDNA targets labeled with AP-Fast Red. However, the AP-Fast Red channel was associated with significant background fluorescence.

We hypothesized that a duplex chromogenic kit with two HRP endpoints could be used to detect vRNA with TSA-fluorescent labels, while vDNA could be visualized with HRP-based non-fluorescent chromogenic labels or TSA-fluorescent labels. Therefore, a custom RNAscope assay, based on ACD's 2.5 chromogenic duplex kit, was developed, substituting the AP endpoint with a second HRP endpoint. Importantly, to accomplish two-step HRP-based staining, an HRP blocking step was included between vRNA and vDNA signal development. Using this approach, we were able to use IF to phenotype vRNA and vDNA positive cells on a single slide from HIV-infected Thy/Liv tissue (Fig. 5). Figures 5A–F show a single Thy/Liv tissue section stained with mIFISH for vDNA (chromogenic ISH) (5A), DAPI (5B), CD3 (IF) (5C), CD163/CD68 (IF) (5C), vRNA (fluorescent ISH) (5E), and an overlay of vRNA, CD3, CD163/CD68, and DAPI (5F). Overlap analysis of digitally aligned vDNA-ISH, vRNA-ISH, CD3-IF, and CD68/CD163-IF images showed that (1) vDNA signal was identified only within the CD3⁺ but not in the CD68/CD163⁺ compartment, (2) vRNA signal was present in both CD3⁺ and CD68/CD163⁺ cells, (3) only a minority of the vRNA⁺ cells co-expressed vDNA, and that (4) a small but sizable proportion of the vRNA⁺ cells could not be positively identified by the immunophenotypical markers (CD3 and CD68/CD163) applied.

The Characterization of the Tissue Burden of HIV Using mIFISH in Human Tissues

FFPE lymph nodes of an HIV-infected viremic patient who was not actively using antiretroviral therapy (ART) were tested for the applicability of mIFISH to assess the tissue burden of HIV in clinical samples. The majority of a vRNA signal was seen within the germinal centers in a reticular pattern reminiscent of the follicular dendritic cell (FDC) network that stains positive for CD21 (Supplemental Fig. 2). The reticular pattern of vRNA distribution is consistent with the notion that free virions produced by infected cells may be attached to the surface of FDCs. In addition, a few dense clusters of vRNA outside the FDC network with the size and shape of single cells were also detected. Next, we applied our mIFISH technology to phenotypically characterize the cells harboring provirus (i.e., vDNA) and those expressing vRNA (Figs. A–K). The reticular pattern of vRNA co-localized with CD21, a marker of FDCs (Fig. 6D–F, purple arrows), and this was distinguishable from vRNA associated with CD3⁺ T-cells (Fig. 6A–D, red arrow). In addition, in the same tissue section, we were able to phenotype cells harboring the provirus as being CD3⁺ T-cells (Fig. 6A, black circles

and 6B–C: white circles). Interestingly, rare CD68/CD163⁺ macrophages also expressed vRNA (Fig. 6G–K, yellow arrow), as shown in a separate section stained for DAPI (6G), CD3 (IF) (6H), vRNA (fluorescent ISH) (6I), CD68/CD163 (IF) (6J), and overlay of vRNA (fluorescent ISH) + IF (6K). Control lymph nodes from HIV⁻ patients showed negligible background staining with ISH vRNA (data not shown).

Assessment of the Quantitative Aspects of RNAscope for vRNA

We also sought to independently assess the quantitative nature of the vRNA-ISH assay using qPCR. Two lymph nodes from a single HIV-infected viremic patient who was not on ART at the time of the biopsies were selected for testing. Samples designated A and B were obtained six days apart, and the plasma HIV viral load on the day of the first biopsy was 114,606 copies/ml. Image analysis was applied to quantitate the vRNA-ISH signal in tissue sections using Definiens Tissue Studio software. Of all the cells in the lymph nodes, 2.1% and 7.6% of the cells were positive for vRNA in samples A and B, respectively (Fig. 7A). Of the cells with detectable HIV-RNA, those with a single dot signal were the most common (1.7% in sample A and 4.2% in sample B) while the prevalence of cells with two to five dots was 0.3% and 2%, respectively. Finally, cells with large fused cytoplasmic clusters of vRNA surrounding the nuclei, representing many transcripts, made up 0.2% and 1.3% of cells in lymph nodes A and B, respectively. Negative controls showed no detectable vRNA signal in either sample. For quantitative assessment of the viral (vRNA) load, the following assumptions were made: (1) the smallest visible punctate signal represents the smallest amount of vRNA detectable by the RNAscope ISH assay, and that (2) larger dots and confluent signals represent proportionally larger quantities of viral transcripts. First, the mean size of the individual punctate dots was calculated using Tissue Studio software (Definiens) from a total of 249,854 single dots [mean = 1.19 μm^2 , range = 0.3–8 μm^2 , designated as mean unit value (MUV)] and then measured the total area of vRNA⁺ signal in μm^2 . By dividing the total area of vRNA⁺ signal with the MUV, we were able to estimate the quantity of the vRNA signal as a measure of the number of MUVs in the section. The number of HIV transcript MUV in a given 4- μm section of tissue was 56,178 and 247,703 from samples A and B, respectively (Fig. 7B). The procedure was repeated three times on three separate days using two whole-slide images with identical results on all 3 days. We then compared QIA findings with qPCR results performed on the corresponding FFPE tissue

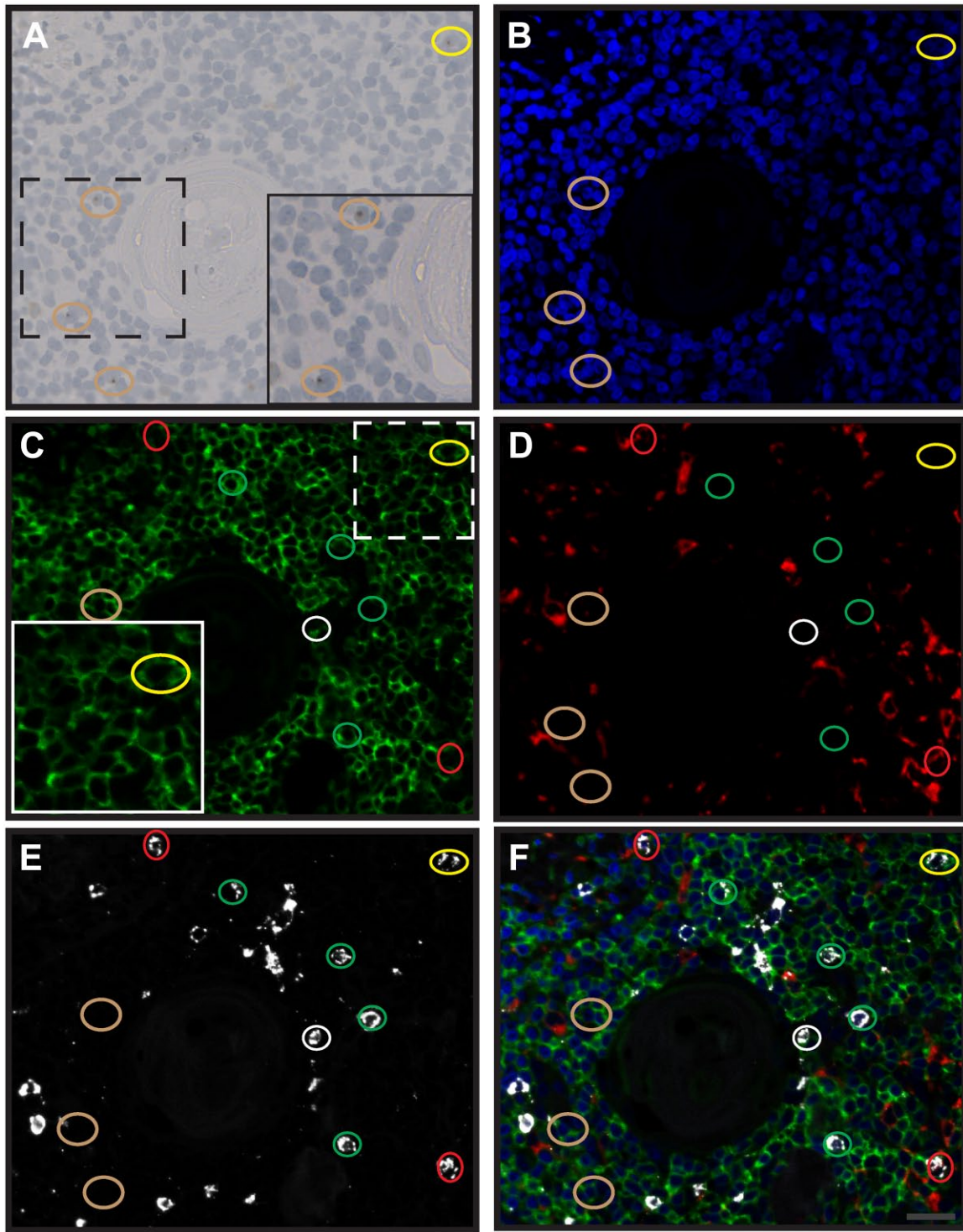
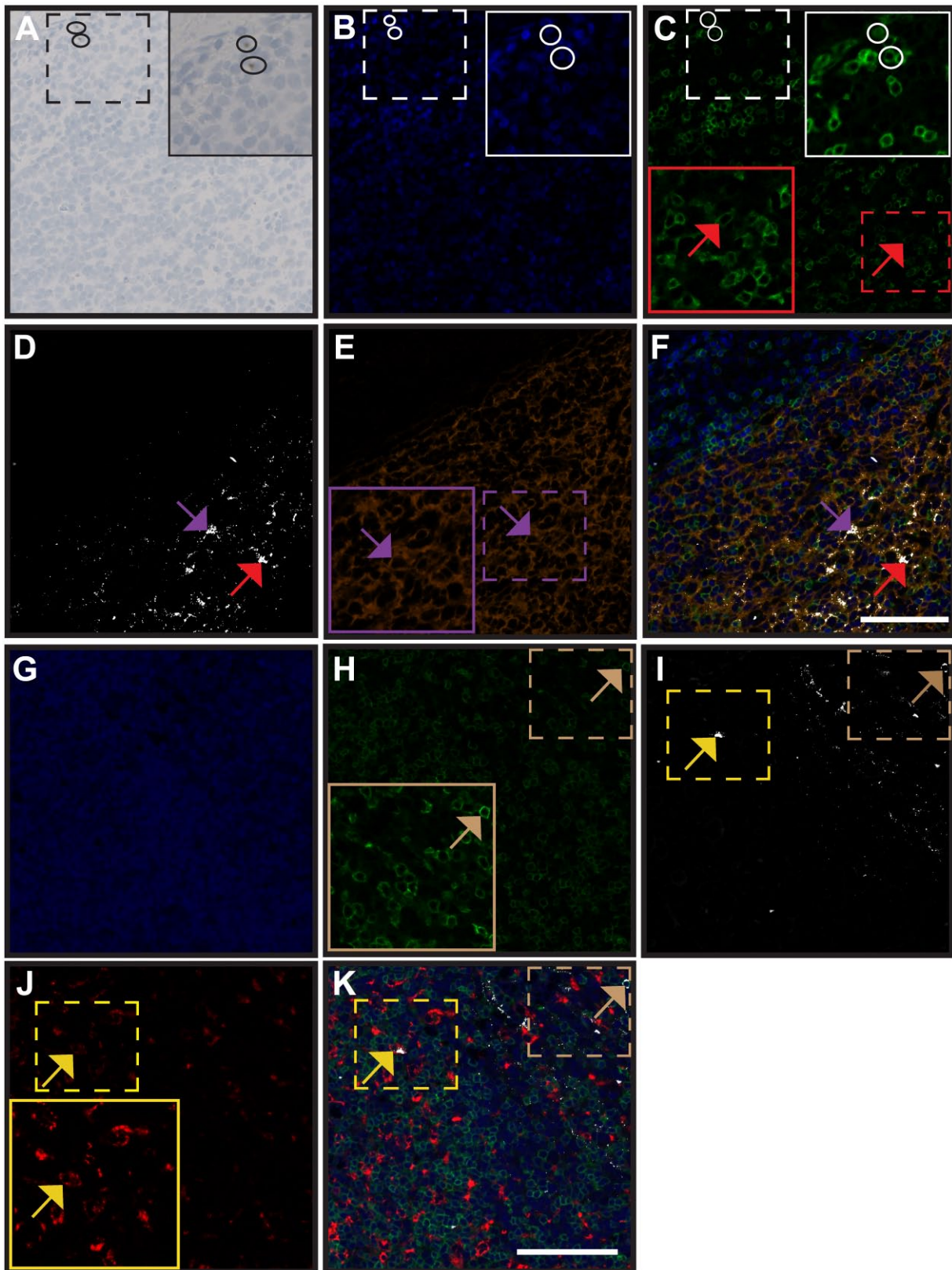


Figure 5. Multiplexed phenotyping of vRNA and vDNA positive cells in Thymus/Liver tissues with chromogenic + fluorescent mFISH. To use multi-marker immunofluorescence for phenotypical assessment along with vDNA and vRNA, a novel duplex RNAscope assay was developed with two HRP endpoints allowing for the multiplexed detection of chromogenic (vDNA) ISH signal by DAB and fluorescent (vRNA) ISH signal using TSA-fluorescence. To phenotypically assess vDNA⁺ cells, bright-field images stained for vDNA (DAB-brown) and with hematoxylin counterstain (blue) (A) were overlaid with images of the same section using fluorescence-based detection—DAPI (blue, B); CD3 (green, IF, C); CD68/CD163 (red, IF, D); vRNA (white, TSA-fluorescence, E); and overlay (F). The brown circles and yellow circle highlight a vDNA⁺/vRNA⁻/CD3⁺ and vDNA⁺/vRNA⁺/CD3⁺ cells, respectively. The green circles show vRNA⁺/CD3⁺ cells, and the red circle shows a vRNA⁺/CD68⁻CD163⁺ cell. Rare cells that cannot be identified by the CD3/CD68/CD163 phenotypical markers are shown in white circles. Scale bar = 20 μm. Abbreviations: vRNA, HIV-RNA; vDNA, HIV-DNA; mFISH, multiplexed IF and ISH; DAB, 3,3' diaminobenzidine tetrahydrochloride; HRP, horseradish peroxidase; ISH, in situ hybridization; DAPI, 4',6-diamidino-2-phenylindole; IF, immunofluorescence; TSA, tyramide signal amplification.



(continued)

Figure 6. Multiplexed phenotyping of vRNA and vDNA positive cells in human lymph node with chromogenic + fluorescent mFISH. Two FFPE sections from a single HIV⁺ human rectal biopsy were stained with a novel duplex RNAscope assay with two HRP endpoints. Both sections were stained for vDNA (DAB-brown) and with hematoxylin counterstain (blue, A); DAPI (blue, B and G); CD3 (green, IF, C and H); vRNA (white, TSA-fluorescence, D and I). In addition, one section was stained with CD21 (orange, fluorescent, A–F), while the other section was stained with CD68/CD163 (red, fluorescent, G–K). To phenotypically assess vDNA⁺ cells, bright-field images stained for vDNA with DAB-brown and hematoxylin-blue (A) were overlaid with images using fluorescence-based detection of IF markers (B–F). Black and white circles in A–C highlight vDNA⁺/CD3⁺ cells. In panels C–F, red and purple arrows highlight vRNA (D, white) associated with CD3⁺ cells (C, green) and CD21⁺ cells (C, orange), respectively. The CD21⁺ cells (C, orange) are in a reticular pattern consistent with the FDC network. Then, on a separate tissue section, in G–K, yellow and brown arrows indicate a vRNA⁺ cell that was phenotyped as CD68/CD163⁺ or CD3⁺, respectively. Scale bar = 100 μ m. Abbreviations: vRNA, HIV-RNA; vDNA, HIV-DNA; mFISH, multiplexed IF and ISH; FFPE, formalin-fixed paraffin-embedded; DAB, 3,3'-diaminobenzidine tetrahydrochloride; HRP, horseradish peroxidase; DAPI, 4',6-diamidino-2-phenylindole; IF, immunofluorescence; FDC, follicular dendritic cell; TSA, tyramide signal amplification.

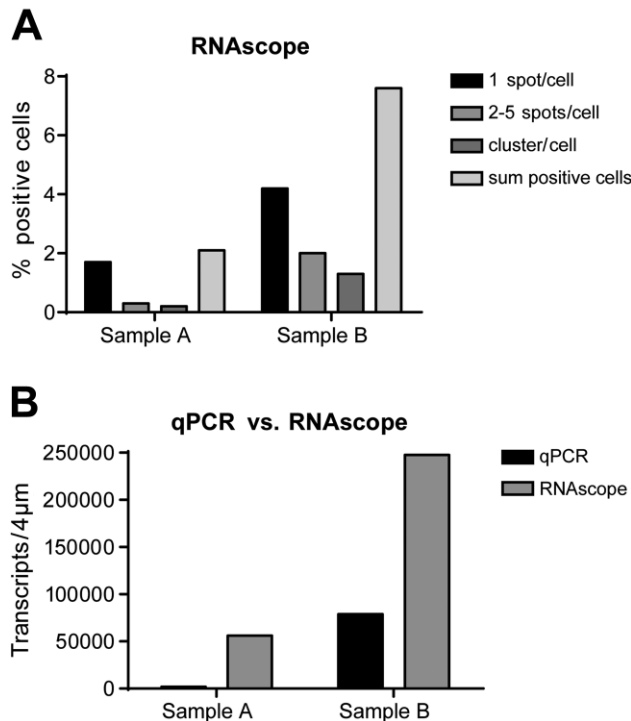


Figure 7. Comparing ISH (RNAscope) with qPCR for the quantitation of tissue-associated vRNA in FFPE tissues. Panel A: Quantitation of ISH (RNAscope) signal using Definiens Tissue Studio image analysis software. Single-cell quantitative analysis of vRNA signal was performed on whole-slide digital images of FFPE sections from two separate lymph nodes obtained from the same HIV⁺ donor 6 days apart. Image analysis revealed less vRNA signal in sample A compared with sample B. Cells with only one signal per cell represent the largest fraction of HIV⁺ cells when compared with cells with two to five signals or those with larger clusters of signals. Panel B: Both qPCR performed on RNA isolated from FFPE sections and whole-slide digital imaging analysis of RNAscope signal indicate a higher number of vRNA transcripts in sample B compared with sample A. Abbreviations: ISH, in situ hybridization; vRNA, HIV-RNA; qPCR, quantitative polymerase chain reaction; FFPE, formalin-fixed paraffin-embedded.

sections on samples A and B. As an internal control, we isolated RNA from one 10- μ m section and from two 10- μ m sections from each tissue and performed qPCR

in duplicate on each of two samples from both lymph nodes. The quantity of vRNA correlated with the number of tissue sections used for the RNA isolation, that is, more vRNA was found from qPCR performed on RNA isolated from two 10- μ m sections versus one. After normalizing the vRNA for section thickness, the number of vRNA MUVs was higher with ISH (RNAscope) than the quantity of vRNA measured by qPCR. Both techniques identified higher numerical vRNA values in sample B (Tissue A: qPCR = 1813, RNAscope = 56,178; Tissue B: qPCR = 78,960, RNAscope = 247,703; Fig. 7B) than sample A. These data indicate that quantitative measurements of vRNA from tissue sections by ISH (RNAscope) and qPCR are concordant; the higher MUVs of vRNA by RNAscope may indicate higher sensitivity of ISH than qPCR in FFPE specimens.

Discussion

The elusive nature of assessing the tissue reservoirs of HIV is one of the major impediments of cure. Development of highly sensitive technologies that can identify individual cells harboring HIV nucleic acids in situ in tissue sections is the prerequisite for successful tissue-based investigative studies of HIV research in humans. Herein we describe, for the first time, a mFISH assay for (1) in situ quantitative assessment of individual cells harboring HIV-RNA and for (2) phenotypic characterization of the HIV-RNA⁺ and HIV-vDNA⁺ cells in FFPE human tissues. Optimized protocols for pre-analytical variables of tissue collection, fixation, and processing are also presented. Finally, we describe an image analysis protocol for HIV vRNA-ISH signal quantitation on whole-slide digital images.

Currently, tissue-based multiplexed ISH and IF technologies seem to be the most feasible approach to detect virally infected cells combined with phenotypic analysis. The work by Deleage et al. in non-human primates indicates that the RNAscope platform may offer superior sensitivity and specificity compared with

other ISH methods.¹⁰ However, to further improve the utility of this technique, we sought to optimize the pre-analytical variables of tissue fixation and processing and to extend the test's ability to phenotypically identify subsets of cells harboring HIV nucleic acids. Our work, which assessed several fixatives, is in line with previous findings that formalin is an important component of fixation for ISH as we demonstrated that only those tissues fixed in formalin-containing fixatives showed positive ISH reaction.^{12,15}

Our results indicate that fixation time and exposure to ethanol before processing and paraffin embedding were important factors for successful ISH. The findings from Thy/Liv tissues and human rectal biopsies demonstrating poor ISH staining in tissues that had been exposed to ethanol for an extended period of time (days to weeks) are in line with previous work suggesting that alcohol-based fixatives may hydrolyze formaldehyde-induced cross-links, thereby partially reversing fixation or that RNA targets may precipitate out of tissues when exposed to ethanol, resulting in degradation-disappearance of RNA targets.^{15,24,25} Interestingly, Thy/Liv samples fixed in 4% PFA and then exposed to ethanol for 24–48 hr demonstrated improved ISH signal if the PFA fixation temperature was increased from 4C to room temperature or if PFA fixation time was increased from 1 to 3 days. Yet, tissues exposed to ethanol for ≥ 24 hr after fixation with formalin showed inferior ISH staining compared with samples that did not undergo prolonged exposure to ethanol. In addition to fixation, other factors, such as storage conditions of the FFPE blocks and time in storage may also contribute to RNA degradation, the impact of which was not addressed in our experimental design. Ultimately, the optimal fixation for HIV-ISH on Thy/Liv tissues was found to be freshly made 4% PFA for 3 days at 4C followed by immediate dehydration in graded ethanol and paraffin embedding, with no prolonged ethanol exposure. In keeping with previous observations, these data indicate that PFA cross-linking is a necessary component of RNA-ISH and that formaldehyde is superior to alcohol fixation for RNA-ISH.^{12,15,26}

Our next goal was to build a platform for multiplexed phenotypic assessment of cells positive for vRNA and vDNA. Chromogenic staining of viral nucleic acids is appealing given the ease of assessment by bright-field microscopy and the potential for enzyme-based signal amplification compared with fluorescent-based methods. However, chromogenic staining has limitations in the setting of single-cell analysis when considering the number of markers that can be distinguished using different colors on the same cell. Therefore, we turned to a multiplexed approach in which small vDNA signals

were identified using chromogenic stains and more abundant vRNA and phenotypic protein targets were identified by fluorescence. Importantly, this approach, along with TSA-fluorescence, allowed us to overcome the optical barrier that prominent chromogenic precipitates pose to concurrent fluorescent signals. Using these newly established techniques, we were able to perform multiplexed analysis of individual cells positive for vDNA and vRNA with multiple immunophenotypic markers on HLN and gut biopsies from viremic patients not actively using ART. The vRNA signal by ISH showed three predominant patterns in all viremic human tissues. Cells with confluent vRNA signal; smaller punctate dots that may represent putative viral particles, as described by Deleage et al.; and dense punctate dots present in a reticular pattern indicative of FDC associated virus.^{6,9,10} Cells with confluent signal in HLN from viremic donors and in Thy/Liv tissues from humanized mice were phenotyped as CD3⁺ T-cells or CD163/CD68⁺ macrophages, with infected T-cells greatly outnumbering macrophages in all tissues studied. As expected, the reticular-pattern vRNA signal co-localized with the FDC marker CD21. Interestingly, while all vRNA⁺ cells would be expected to harbor integrated HIV-DNA, cells staining vRNA⁺/vDNA⁻ by RNAscope were a common occurrence. This is likely due to nuclei assessed in cross section, decreased accessibility of HIV-DNA compared with HIV-RNA to ISH probes, or an overall decreased sensitivity of the RNAscope for vDNA compared with vRNA.

Finally, we attempted to quantitate the RNAscope HIV-RNA signal using QIA and compare it with qPCR performed on tissues from the corresponding FFPE blocks. For QIA of the vRNA, we have developed a novel, simple, and highly reproducible protocol that will also be applicable for other RNAscope assays. In the two HLN assessed, we found that the two independent methods of HIV-RNA analysis were qualitatively concordant. Although the image analysis data are quantitative and highly reproducible, the precise number of actual viral RNA cannot be inferred from these data without solid evidence for the sensitivity of the RNAscope assay for *in situ* HIV-RNA detection.

Herein, we describe the use of mFISH to phenotypically define the tissue burden of HIV *in situ*. There are several limitations when considering the generalizability of these methods. The techniques described were optimized in Thy/Liv tissues and found to be successful in HLN and human gut tissues. However, some level of optimization may be required in different tissues. In addition, our study did not include an exhaustive list of potential fixatives or conditions. Therefore, the fixatives found to be suboptimal in our study may

have had improved results under different conditions, and different fixatives may have provided improved ISH results. Also, the conditions for fixation and tissue preparation described above were optimized for HIV-RNA and HIV-DNA ISH and not necessarily for immunophenotyping. Thus, target antigens may be best visualized by different tissue preparation conditions, antibodies, or staining methods. It should be noted that these methods were developed in tissues from sources with a high plasma viral load. Thus, the interpretation of the vDNA signal is dependent on background levels seen in HIV⁻ controls and may be limited in tissues from ART-suppressed individuals who are expected to have rare events. Therefore, staining and analysis of many sections of tissue from an individual donor may be required to reliably quantify and characterize tissue HIV reservoirs. Such an assessment may be costly, time-consuming, prone to error, and may benefit from an automated staining approach. Moreover, the single-cell analysis of multiplexed chromogenic and fluorescent signals requires a labor-intensive pixel-to-pixel overlay of regions of interest from bright-field and fluorescent images taken by two different cameras with variability in pixel data, making such an assessment on many slides per sample cumbersome. Unfortunately, algorithms for rapid whole-slide assessment of multiplexed chromogenic and fluorescent signals are not readily available. The characterization of a rare event, such as HIV reservoirs or a tumor cell, will require a high-throughput approach. Flow cytometry has proven to fill this role for cell suspensions but techniques for whole tissue analysis are lacking. Thus, for in situ technologies to be useful in this context, significant advances must be made at every step to decrease costs and to increase speed and reproducibility; for example, standardized tissue preparation, automated staining, whole-slide scanning, and automated whole-slide quantitative analysis. As high-throughput methods to analyze nucleic acids from fixed and banked tissues are developed, it will be important that we preserve tissues in a manner that provides the highest likelihood of success. Our work provides a standardized approach for tissue preparation that can be used to preserve HIV-infected tissues for the downstream multiplexed analysis of HIV nucleic acids by RNAscope ISH and immunophenotyping by IF.

Acknowledgments

The authors thank the Stoddart lab especially; Mary Beth Moreno, Sofiya Galkina, Jose Rivera, and Galina Kosikova for providing the Thymus/Liver tissues used in this study; Jarish Cohen, for performing the RNA isolation that was used in qPCR studies; the Molecular Imaging Center facility at the Cancer Research Laboratory at University of California

(UC) Berkeley, where the microscopy images were taken; and especially Jen-Yi Lee for assistance with the microscopy.

Competing Interests

The author(s) declared no potential conflicts of interest with respect to the research, authorship, and/or publication of this article.

Author Contributions

All authors have contributed to this article as follows: JJV conceived, designed, and coordinated research studies; conducted experiments, analyzed data, and wrote the manuscript. RH designed and conducted experiments; analyzed data, and created the figures. BA-R conducted experiments and analyzed data. HJ conducted experiments and analyzed data. DD conducted experiments and analyzed data. JM conceived, designed, and coordinated research studies; analyzed data; and edited the manuscript. PWH conceived, designed, and coordinated research studies; analyzed data; and edited the manuscript. CAS designed and coordinated research studies, and edited the manuscript. TJH designed and conducted experiments, and analyzed data. CT conducted experiments. EG conducted experiments. LEH conducted experiments. ZGL conceived, designed, and coordinated research studies; analyzed data; and edited the manuscript. All authors have read and approved the final manuscript.

Funding

The author(s) disclosed receipt of the following financial support for the research, authorship, and/or publication of this article: This work was supported by the National Institutes of Health (UM1AI126611, U19AI096109, R21AI116295, U24AI118675); AIDS and Cancer Specimen Resource Young Investigator Pilot Award (National Cancer Institute; UM1 CA181255); the Deutsche Forschungsgemeinschaft (KFO 243); and the amfAR Institute for HIV Cure, with funding from amfAR grant number 109301.

Human and Animal Study Compliance

The work on animals followed institutional, local, and national guidelines for animal experimentation and was approved by an institutional review board (IRB) and supported in part with federal funds from National Institute of Allergy and Infectious Diseases (NIAID), National Institutes of Health (NIH), under contract number HHSN272201400002C. The work on human subjects was performed in accordance with the principles of the Helsinki Declaration of 1975 and was approved by the University of California, San Francisco (UCSF) Committee on Human Subjects Research, and all participants provided informed consent. The UCSF SCOPE cohort provided a source of rectal biopsies, and lymph nodes were collected under IRB protocol number 14-13840. All work was supported with the NIH grants listed above.

ORCID iDC Thanh  <https://orcid.org/0000-0001-6458-3469>**Literature Cited**

- Chun TW, Moir S, Fauci AS. HIV reservoirs as obstacles and opportunities for an HIV cure. *Nat Immunol*. 2015;16(6):584–9.
- Churchill MJ, Deeks SG, Margolis DM, Siliciano RF, Swanstrom R. HIV reservoirs: what, where and how to target them. *Nat Rev Microbiol*. 2016;14(1):55–60.
- Wong JK, Yukl SA. Tissue reservoirs of HIV. *Curr Opin HIV AIDS*. 2016;11(4):362–70.
- Fletcher CV, Staskus K, Wietgreffe SW, Rothenberger M, Reilly C, Chipman JG, Beilman GJ, Khoruts A, Thorkelson A, Schmidt TE, Anderson J, Perkey K, Stevenson M, Perelson AS, Douek DC, Haase AT, Schacker TW. Persistent HIV-1 replication is associated with lower anti-retroviral drug concentrations in lymphatic tissues. *Proc Natl Acad Sci U S A*. 2014;111(6):2307–12.
- Banga R, Procopio FA, Noto A, Pollakis G, Cavassini M, Ohmiti K, Corpataux JM, de Leval L, Pantaleo G, Perreau M. PD-1(+) and follicular helper T cells are responsible for persistent HIV-1 transcription in treated aviremic individuals. *Nat Med*. 2016;22(7):754–61.
- Fukazawa Y, Lum R, Okoye AA, Park H, Matsuda K, Bae JY, Hagen SI, Shoemaker R, Deleage C, Lucero C, Morcock D, Swanson T, Legasse AW, Axthelm MK, Hesselgesser J, Geleziunas R, Hirsch VM, Edlfsen PT, Piatak M Jr, Estes JD, Lifson JD, Picker LJ. B cell follicle sanctuary permits persistent productive simian immunodeficiency virus infection in elite controllers. *Nat Med*. 2015;21(2):44–51.
- Hurst J, Hoffmann M, Pace M, Williams JP, Thornhill J, Hamlyn E, Meyerowitz J, Willberg C, Koelsch KK, Robinson N, Brown H, Fisher M, Kinloch S, Cooper DA, Schechter M, Tambussi G, Fidler S, Babiker A, Weber J, Kelleher AD, Phillips RE, Frater J. Immunological biomarkers predict HIV-1 viral rebound after treatment interruption. *Nat Commun*. 2015;6:8495.
- Vallejo A. HIV-1 reservoir association with immune activation. *EBioMedicine*. 2015;2(9):1020–1.
- Schacker T, Little S, Connick E, Gebhard K, Zhang ZQ, Krieger J, Pryor J, Havlir D, Wong JK, Schooley RT, Richman D, Corey L, Haase AT. Productive infection of T cells in lymphoid tissues during primary and early human immunodeficiency virus infection. *J Infect Dis*. 2001;183(4):555–62.
- Deleage C, Wietgreffe SW, Del Prete G, Morcock DR, Hao XP, Piatak M, Bess J, Anderson JL, Perkey KE, Reilly C, McCune JM, Haase AT, Lifson JD, Schacker TW, Estes JD. Defining HIV and SIV reservoirs in lymphoid tissues. *Pathog Immun*. 2016;1(1):68–106.
- Maidji E, Somsouk M, Rivera JM, Hunt PW, Stoddart CA. Replication of CMV in the gut of HIV-infected individuals and epithelial barrier dysfunction. *PLoS Pathog*. 2017;13(2):e1006202.
- Stylianopoulou E, Lykidis D, Ypsilantis P, Simopoulos C, Skavdis G, Grigoriou M. A rapid and highly sensitive method of non radioactive colorimetric in situ hybridization for the detection of mRNA on tissue sections. *PLoS ONE*. 2012;7(3):e33898.
- Tbakhi A, Totos G, Hauser-Kronberger C, Pettay J, Baunoch D, Hacker GW, Tubbs RR. Fixation conditions for DNA and RNA in situ hybridization: a reassessment of molecular morphology dogma. *Am J Pathol*. 1998;152(1):35–41.
- Basyuk E, Bertrand E, Journot L. Alkaline fixation drastically improves the signal of in situ hybridization. *Nucleic Acids Res*. 2000;28(10):E46.
- Yan F, Wu X, Crawford M, Duan W, Wilding EE, Gao L, Nana-Sinkam SP, Villalona-Calero MA, Baiocchi RA, Otterson GA. The search for an optimal DNA, RNA, and protein detection by in situ hybridization, immunohistochemistry, and solution-based methods. *Methods*. 2010;52(4):281–6.
- Srinivasan M, Sedmak D, Jewell S. Effect of fixatives and tissue processing on the content and integrity of nucleic acids. *Am J Pathol*. 2002;161(6):1961–71.
- Hewitt SM, Baskin DG, Frevert CW, Stahl WL, Rosamolinar E. Controls for immunohistochemistry. *J Histochem Cytochem*. 2014;62(10):693–7.
- Malnati MS, Scarlatti G, Gatto F, Salvatori F, Cassina G, Rutigliano T, Volpi R, Lusso P. A universal real-time PCR assay for the quantification of group-M HIV-1 proviral load. *Nat Protoc*. 2008;3(7):1240–8.
- Henrich TJ, Gallien S, Li JZ, Pereyra F, Kuritzkes DR. Low-level detection and quantitation of cellular HIV-1 DNA and 2-LTR circles using droplet digital PCR. *J Virol Methods*. 2012;186(1–2):68–72.
- O'Doherty U, Swiggard WJ, Jeyakumar D, McGain D, Malim MH. A sensitive, quantitative assay for human immunodeficiency virus type 1 integration. *J Virol*. 2002;76(21):10942–50.
- Symons J, Chopra A, Malatinkova E, De Spiegelaere W, Leary S, Cooper D, Abana CO, Rhodes A, Rezaei SD, Vandekerckhove L, Mallal S, Lewin SR, Cameron PU. HIV integration sites in latently infected cell lines: evidence of ongoing replication. *Retrovirology*. 2017;13(1):2.
- Bussolati G, Annaratone L, Medico E, D'Armento G, Sapino A. Formalin fixation at low temperature better preserves nucleic acid integrity. *PLoS ONE*. 2011;6(6):e21043.
- Karlsson C, Karlsson MG. Effects of long-term storage on the detection of proteins, DNA, and mRNA in tissue microarray slides. *J Histochem Cytochem*. 2011;59(12):1113–21.
- Fowler CB, O'Leary TJ, Mason JT. Modeling formalin fixation and histological processing with ribonuclease A: effects of ethanol dehydration on reversal of formaldehyde cross-links. *Lab Invest*. 2008;88(7):785–91.
- Walker SE, Lorsch J. RNA purification—precipitation methods. *Methods Enzymol*. 2013;530:337–43.
- Matsuda Y, Fujii T, Suzuki T, Yamahatsu K, Kawahara K, Teduka K, Kawamoto Y, Yamamoto T, Ishiwata T, Naito Z. Comparison of fixation methods for preservation of morphology, RNAs, and proteins from paraffin-embedded human cancer cell-implanted mouse models. *J Histochem Cytochem*. 2011;59(1):68–75.